Supporting Information

Glasser et al. 10.1073/pnas.1101141108

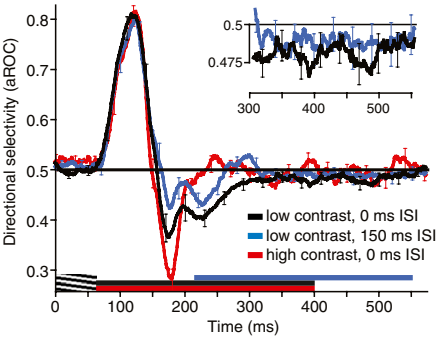

Fig. S1. aROC analysis computed from unfiltered spike counts using a 50-ms sliding window, supplementing the analysis shown in Fig. 5. This analysis explicitly separates the directional off-response (caused by the transient off-response to the null direction and modulated by the onset of the test stimuli) from the sustained response to the test stimuli. The graphic just above the *x* axis illustrates the time courses of three conditions differing in the onset timing (0 vs. 150 ms ISI) and contrast (low vs. high) of the test stimulus. All conditions start with 67 ms of motion adaptation. *Inset*: Close-up of sustained null direction selectivity to low-contrast test stimuli (0 and 150 ms ISI). For clarity, error bars (SEM) are shown every 30 ms. As can be seen from the data, the directional off-response is by far the strongest in the high-contrast test condition (red curve). Importantly, this is also the condition in which (*i*) we find no sustained directional selectivity, (*ii*) our model of the temporal integration of brief motion signals yields no evidence for the null-direction selectivity (Fig. 5*D*, *Middle*), and (*iii*) we find no evidence for MAEs in human observers (Fig. 4). Overall, this indicates that the off-responses cannot explain sustained null-direction selectivity to stationary test stimuli. Our model of temporal integration (Fig. 5) was based on behavioral (1) and neurophysiological (2, 3) evidence that processing of brief motion signals has an obligatory low-pass character. A comparison of the present analysis with the results shown in Fig. 5 illustrates that the low-pass nature of the temporal integration model smooths over brief directional off-responses. By using the analysis detailed in the present study, we analyzed the total duration of each neuron's null-direction selectivity over a 250-ms time window starting after the end of the transient off-response [here defined as the time point (267 ms) at which the result from the 150-ms ISI condition crosses the 0.5 aROC line; note that the results for the 150-ms ISI condition can be used to reveal the effect of the motion offset without the succeeding test stimulus]. Paralleling results in the text, the total duration of null-direction selectivity was significantly longer than expected by chance for neurons tested with low-contrast test stimuli (average of 23 ms; $P < 0.001$) and nonsignificant when the test stimulus was high-contrast (6 ms, $P = 0.4$). The analogous analysis for the 150-ms ISI condition (using a 250-ms window starting 80 ms after the onset of the test stimulus) also yielded a significant result (10 ms, $P = 0.013$). Importantly, this analysis matches that reported in the text and shows significant null-direction selectivity only for the low-contrast test conditions.

1. Simpson WA (1994) Temporal summation of visual motion. *Vision Res* 34:2547–2559.
2. Cook EP, Maunsell JHR (2002) Dynamics of neuronal responses in macaque MT and VIP during motion detection. *Nat Neurosci* 5:985–994.
3. Masse NY, Cook EP (2010) Behavioral time course of microstimulation in cortical area MT. *J Neurophysiol* 103:334–345.

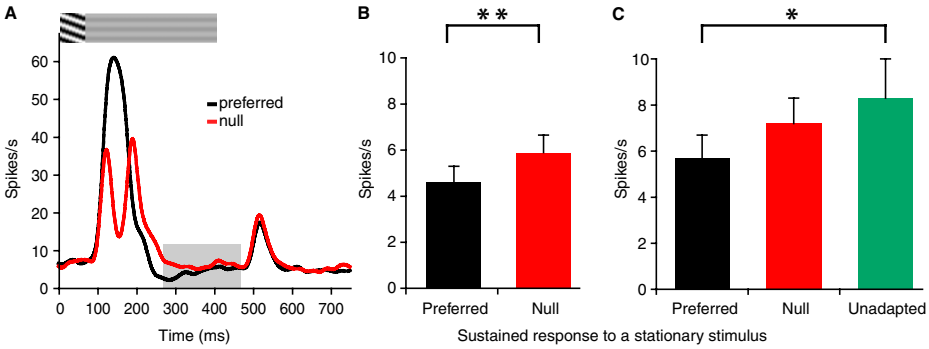

Fig. S2. Spike rate analysis of neural responses to stationary test stimuli. (*A*) Average neural responses (n = 38) to 67 ms of grating motion in the preferred (black) and null (red) directions, followed by a low-contrast stationary test stimulus. Neural activity is shown as firing rates as a function of time (obtained by convolving raw spikes with a Gaussian filter of σ = 10 ms). *Inset*: Space–time plot of the stimulus time course. Shaded area over the x axis indicates a 200-ms widow spanning the sustained response to the stationary test stimulus. The beginning of the window was set to coincide with the end of the transient off-response (Fig. S1). (*B*) Average neural activity (n = 38) during the sustained response to a stationary stimulus (as defined in *A*) following preferred (black) or null (red) motion adaptation. The difference between conditions was significant for both raw spike counts (P = 0.01) and peak rate-normalized activity (P = 0.01). Analogous analysis applied to the high-contrast test condition yielded nonsignificant results (raw, P = 0.55; normalized, P = 0.63), whereas the results were marginally significant for the 150-ms ISI condition (raw, P = 0.08; normalized, P = 0.01). These results are consistent with the key results reported in the text (Fig. 5 *D* and *E*). (C) For a subset of neurons in the main condition (22 of 38), we also recorded responses to stationary stimuli in isolation (i.e., without earlier adaptation to motion). One complication was that stimuli in that experiment were shown at 2% and 4% contrast. To obtain an estimate of responses for 3% contrast stimuli, we log-linearly interpolated between 2% and 4% contrast responses. [Given known nonlinearities at very low contrasts (1), which means any estimation error would cause a slight underestimation of 3% contrast responses. To check whether this would have any effects on the results, we repeated the described analysis using responses to stationary 4% contrast stimuli. The pattern of results, however, did not change. Namely, the only significant difference was a decrease of responses to stationary stimuli following preferred motion adaptation (Tukey honestly significant difference test, P = 0.02).] Next, we compared the sustained part of these responses (starting at 150 ms after the stimulus onset) to the sustained responses of the same neurons to stationary stimuli following preferred (black) or null (red) motion adaptation. The results revealed significant differences among means [raw, $F(2,42)$ = 3.33, P = 0.04; normalized, $F(2,42)$ = 3.34, P = 0.04]. The key result is that the responses to stationary stimuli following exposure to preferred motion were lower than the unadapted responses to static stimuli (Tukey honestly significant difference test, P = 0.04). This indicates that null-direction selectivity for the test stimulus was mostly driven by decreased postadaptation preferred-direction responses.

1. Sclar G, Maunsell JH, Lennie P (1990) Coding of image contrast in central visual pathways of the macaque monkey. *Vision Res* 30:1–10.

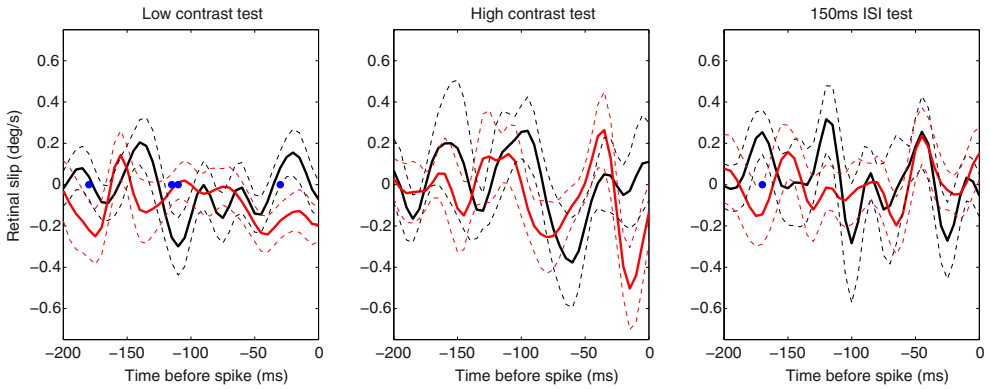

Fig. S3. Spike-triggered eye velocities, which indicate the relationship between small eye movements and neural responses to stationary stimuli following preferred (black) and null (red) motion adaptation. Eye movements were recorded with an EyeLink 1000 tracker at 200Hz (RMS resolution, 0.01°; microsaccade resolution, 0.05°). To extract eye velocity, we first removed line noise from the eye position traces using a 60-Hz notch filter. We then smoothed the position data with a median filter (1) (for the data presented here, we used a 15-ms filter, but the observed results were robust over a wide range of filter widths) and differentiated the resulting traces to estimate eye velocity. Blinks, identified as large velocity transients, were removed. The resulting eye velocity vector at each time point was then projected onto the preferred-null axis of each neuron to obtain a measure of retinal slip that was likely to be associated with neuronal responses. To determine whether these small eye movements could explain the observed differences between postadaptation preferred and null responses, we computed the spike-triggered retinal slip velocity. This analysis measures the average eye velocity that preceded a spike by a given latency, such that any tendency of eye velocity to change firing frequency would be revealed as a peak at the corresponding latency. Spike-triggered retinal slip velocities were computed over a range of latencies covering the 200 ms preceding each spike. This analysis was performed for spikes occurring during time windows in which we found differences following preferred and null adaptation. Specifically, we analyzed spikes in time windows used in the analysis reported in Fig. S1 (results shown earlier) and also for spikes occurring in time windows used in Fig. S2. Before the analysis, the trial-by-trial retinal slips were smoothed by convolving with a Gaussian filter of σ = 8 ms. Filter width was chosen from a range (0, 1, 2 . . . 24, 25) as the one that maximized the number of significant differences between preferred (black line) and null (red line) spike-triggered retinal slips. Under this analysis, modulation of the firing rate by eye movements would appear as an increase in the retinal slip velocity in the preferred or null direction at a specific time (corresponding to neural latency) before the spike. In contrast, the results show no obvious relationship between eye velocity and spike probability. Blue circles show time points at which we found significant differences between preferred and null results (uncorrected $P < 0.05$). The total number of significant time points in the low contrast test condition was smaller than expected by chance alone (permutation test, $P = 0.14$). Analogous analysis for spikes occurring in time windows used in Fig. S2 (i.e., looking only at the sustained responses to stationary test stimuli) yielded a total of two significant time points across all three conditions. Overall, these results show no evidence for a relationship between eye movements and the adaptation effects we report.

1. Hafed ZM, Clark JJ (2002) Microsaccades as an overt measure of covert attention shifts. *Vision Res* 42:2533–2545.

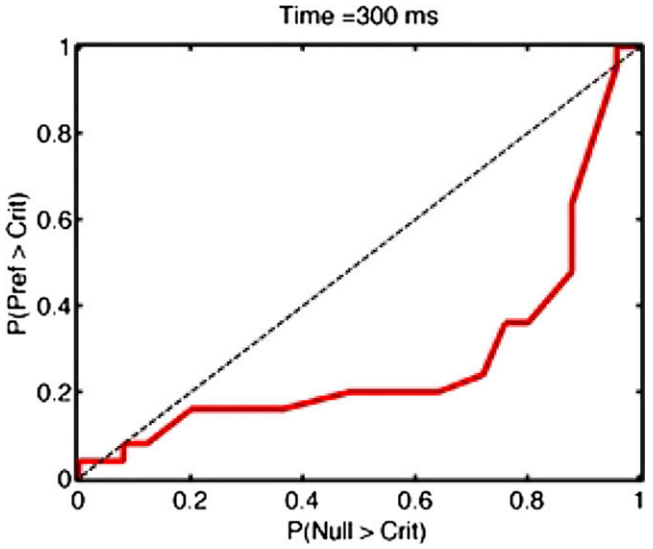

Movie S1. Complete sequence of time-dependent ROC changes for the example neuron shown in Fig. 5C.

Movie S1